three genetic loci with uric acid concentration and risk of gout: a genome-wide association study. Lancet 372:1953-1961

Doring A, Gieger C, Mehta D, Gohlke H, Prokisch H, Coassin S, Fischer G, Henke K, Klopp N, Kronenberg F, Paulweber B, Pfeufer A, Rosskopf D, Volzke H, Illig T, Meitinger T, Wichmann HE, Meisinger C (2008) SLC2A9 influences uric acid concentrations with pronounced sex-specific effects. Nat Genet 40:430-436

Fairbrother WG, Yeh RF, Sharp PA, Burge CB (2002) Predictive identification of exonic splicing enhancers in human genes. Science 297:1007-1013

Gibbs RA, Caskey CT (1987) Identification and localization of mutations at the Lesch-Nyhan locus by ribonuclease A cleavage. Science 236:303-305

Glorieux FH, Rauch F, Plotkin H, Ward L, Travers R, Roughley P, Lalic L, Glorieux DF, Fassier F, Bishop NJ (2000) Type V osteogenesis imperfecta: a new form of brittle bone disease. J Bone Miner Res 15:1650-1658

Glorieux FH, Ward LM, Rauch F, Lalic L, Roughley PJ, Travers R (2002) Osteogenesis imperfecta type VI: a form of brittle bone disease with a mineralization defect. J Bone Miner Res 17:30-38

Goren A, Ram O, Amit M, Keren H, Lev-Maor G, Vig I, Pupko T, Ast G (2006) Comparative analysis identifies exonic splicing regulatory sequences--The complex definition of enhancers and silencers. Mol Cell 22:769-781

Gorlov IP, Gorlova OY, Frazier ML, Amos CI (2003) Missense mutations in hMLH1 and hMSH2 are associated with exonic splicing enhancers. Am J Hum Genet 73:1157-1161

Graessler J, Graessler A, Unger S, Kopprasch S, Tausche AK, Kuhlisch E, Schroeder HE (2006) Association of the human urate transporter 1 with reduced renal uric acid excretion and hyperuricemia in a German Caucasian population. Arthritis Rheum 54:292-300

Hart TC, Gorry MC, Hart PS, Woodard AS, Shihabi Z, Sandhu J, Shirts B, Xu L, Zhu H, Barmada MM, Bleyer AJ (2002) Mutations of the UMOD gene are responsible for medullary cystic kidney disease 2 and familial juvenile hyperuricaemic nephropathy. J Med Genet 39:882-892

Hartikka H, Kuurila K, Korkko J, Kaitila I, Grenman R, Pynnonen S, Hyland JC, Ala-Kokko L (2004) Lack of correlation between the type of COL1A1 or COL1A2 mutation and hearing loss in osteogenesis imperfecta patients. Hum Mutat 24:147-154

Hebsgaard SM, Korning PG, Tolstrup N, Engelbrecht J, Rouze P, Brunak S (1996) Splice site prediction in Arabidopsis thaliana pre-mRNA by combining local and global sequence information. Nucleic Acids Res 24:3439-3452

Ishizuka T, Ahmad I, Kita K, Sonoda T, Ishijima S, Sawa K, Suzuki N, Tatibana M (1996) The human phosphoribosylpyrophosphate synthetase-associated protein 39 gene (PRPSAP1) is located in the chromosome region 17q24-q25. Genomics 33:332-334

Katashima R, Iwahana H, Fujimura M, Yamaoka T, Itakura M (1998) Assignment of the human phosphoribosylpyrophosphate synthetase-associated protein 41 gene (PRPSAP2) to 17p11.2-p12. Genomics 54:180-181

Kolz M, Johnson T, Sanna S, Teumer A, Vitart V, Perola M, Mangino M, Albrecht E, Wallace C, Farrall M, Johansson A, Nyholt DR, Aulchenko Y, Beckmann JS, Bergmann S, Bochud M, Brown M, Campbell H, Connell J, Dominiczak A, Homuth G, Lamina C, McCarthy MI, Meitinger T, Mooser V, Munroe P, Nauck M, Peden J, Prokisch H, Salo P, Salomaa V, Samani NJ, Schlessinger D, Uda M, Volker U, Waeber G, Waterworth D, Wang-Sattler R, Wright AF, Adamski J, Whitfield JB, Gyllensten U, Wilson JF, Rudan I, Pramstaller P, Watkins H, Doering A, Wichmann HE, Spector TD, Peltonen L, Volzke H, Nagaraja R, Vollenweider P, Caulfield M, Illig T, Gieger C (2009) Meta-analysis of 28,141 individuals identifies common variants within five new loci that influence uric acid concentrations. PLoS Genet 5:e1000504

Kumar P, Henikoff S, Ng PC (2009) Predicting the effects of coding non-synonymous variants on protein function using the SIFT algorithm. Nat Protoc 4:1073-1081

Lalonde E, Albrecht S, Ha KC, Jacob K, Bolduc N, Polychronakos C, Dechelotte P, Majewski J, Jabado N (2010) Unexpected allelic heterogeneity and spectrum of mutations in Fowler syndrome revealed by next-generation exome sequencing. Hum Mutat 31:918-923

Langmead B, Trapnell C, Pop M, Salzberg SL (2009) Ultrafast and memory-efficient alignment of short DNA sequences to the human genome. Genome Biol 10:R25

Lapunzina P, Aglan M, Temtamy S, Caparros-Martin JA, Valencia M, Leton R, Martinez-Glez V, Elhossini R, Amr K, Vilaboa N, Ruiz-Perez VL (2010) Identification of a frameshift mutation in Osterix in a patient with recessive osteogenesis imperfecta. Am J Hum Genet 87:110-114

Licatalosi DD, Mele A, Fak JJ, Ule J, Kayikci M, Chi SW, Clark TA, Schweitzer AC, Blume JE, Wang X, Darnell JC, Darnell RB (2008) HITS-CLIP yields genome-wide insights into brain alternative RNA processing. Nature 456:464-469

Lund AM, Schwartz M, Skovby F (1996) Variable clinical expression in a family with OI type IV due to deletion of three base pairs in COL1A1. Clin Genet 50:304-309

Lund AM, Skovby F, Schwartz M (1997) Serine for glycine substitutions in the C-terminal third of the alpha 1(I) chain of collagen I in five patients with nonlethal osteogenesis imperfecta. Hum Mutat 9:378-382

Marini JC, Forlino A, Cabral WA, Barnes AM, San Antonio JD, Milgrom S, Hyland JC, Korkko J, Prockop DJ, De Paepe A, Coucke P, Symoens S, Glorieux FH, Roughley PJ, Lund AM, Kuurila-Svahn K, Hartikka H, Cohn DH, Krakow D, Mottes M, Schwarze U, Chen D, Yang K, Kuslich C, Troendle J, Dalgleish R, Byers PH (2007) Consortium for osteogenesis imperfecta mutations in the helical domain of type I collagen: regions rich in lethal mutations align with collagen binding sites for integrins and proteoglycans. Hum Mutat 28:209-221

McKinney JL, Murdoch DJ, Wang J, Robinson J, Biltcliffe C, Khan HM, Walker PM, Savage J, Skerjanc I, Hegele RA (2004) Venn analysis as part of a bioinformatic approach to prioritize expressed sequence tags from cardiac libraries. Clin Biochem 37:953-960

Morello R, Bertin TK, Chen Y, Hicks J, Tonachini L, Monticone M, Castagnola P, Rauch F, Glorieux FH, Vranka J, Bachinger HP, Pace JM, Schwarze U, Byers PH, Weis M, Fernandes RJ, Eyre DR,

Yao Z, Boyce BF, Lee B (2006) CRTAP is required for prolyl 3- hydroxylation and mutations cause recessive osteogenesis imperfecta. Cell 127:291-304

Mottes M, Sangalli A, Valli M, Gomez Lira M, Tenni R, Buttitta P, Pignatti PF, Cetta G (1992) Mild dominant osteogenesis imperfecta with intrafamilial variability: the cause is a serine for glycine alpha 1(I) 901 substitution in a type-I collagen gene. Hum Genet 89:480-484

Ng SB, Bigham AW, Buckingham KJ, Hannibal MC, McMillin MJ, Gildersleeve HI, Beck AE, Tabor HK, Cooper GM, Mefford HC, Lee C, Turner EH, Smith JD, Rieder MJ, Yoshiura K, Matsumoto N, Ohta T, Niikawa N, Nickerson DA, Bamshad MJ, Shendure J (2010a) Exome sequencing identifies MLL2 mutations as a cause of Kabuki syndrome. Nat Genet 42:790-793

Ng SB, Buckingham KJ, Lee C, Bigham AW, Tabor HK, Dent KM, Huff CD, Shannon PT, Jabs EW, Nickerson DA, Shendure J, Bamshad MJ (2010b) Exome sequencing identifies the cause of a mendelian disorder. Nat Genet 42:30-35

Ng SB, Turner EH, Robertson PD, Flygare SD, Bigham AW, Lee C, Shaffer T, Wong M, Bhattacharjee A, Eichler EE, Bamshad M, Nickerson DA, Shendure J (2009) Targeted capture and massively parallel sequencing of 12 human exomes. Nature 461:272-276

Ohno K, Milone M, Shen X-M, Engel AG (2003) A frameshifting mutation in *CHRNE* unmasks skipping of the preceding exon. Hum Mol Genet 12:3055-3066

Rauch F, Glorieux FH (2004) Osteogenesis imperfecta. Lancet 363:1377-1385

Reese MG, Eeckman FH, Kulp D, Haussler D (1997) Improved splice site detection in Genie. J Comput Biol 4:311-323

Roessler BJ, Nosal JM, Smith PR, Heidler SA, Palella TD, Switzer RL, Becker MA (1993) Human X-linked phosphoribosylpyrophosphate synthetase superactivity is associated with distinct point mutations in the PRPS1 gene. J Biol Chem 268:26476-26481

Roschger P, Fratzl-Zelman N, Misof BM, Glorieux FH, Klaushofer K, Rauch F (2008) Evidence that abnormal high bone mineralization in growing children with osteogenesis imperfecta is not associated with specific collagen mutations. Calcif Tissue Int 82:263-270

Sillence DO, Senn A, Danks DM (1979) Genetic heterogeneity in osteogenesis imperfecta. J Med Genet 16:101-116

Stark K, Reinhard W, Grassl M, Erdmann J, Schunkert H, Illig T, Hengstenberg C (2009) Common polymorphisms influencing serum uric acid levels contribute to susceptibility to gout, but not to coronary artery disease. PLoS One 4:e7729

Tabara Y, Kohara K, Kawamoto R, Hiura Y, Nishimura K, Morisaki T, Kokubo Y, Okamura T, Tomoike H, Iwai N, Miki T (2010) Association of four genetic loci with uric acid levels and reduced renal function: the J-SHIPP Suita study. Am J Nephrol 32:279-286

van Dijk FS, Nesbitt IM, Zwikstra EH, Nikkels PG, Piersma SR, Fratantoni SA, Jimenez CR, Huizer M, Morsman AC, Cobben JM, van Roij MH, Elting MW, Verbeke JI, Wijnaendts LC, Shaw NJ, Hogler W, McKeown C, Sistermans EA, Dalton A, Meijers-Heijboer H, Pals G (2009) PPIB mutations cause severe osteogenesis imperfecta. Am J Hum Genet 85:521-527

Vitart V, Rudan I, Hayward C, Gray NK, Floyd J, Palmer CN, Knott SA, Kolcic I, Polasek O, Graessler J, Wilson JF, Marinaki A, Riches PL, Shu X, Janicijevic B, Smolej-Narancic N, Gorgoni B, Morgan J, Campbell S, Biloglav Z, Barac-Lauc L, Pericic M, Klaric IM, Zgaga L, Skaric-Juric T, Wild SH, Richardson WA, Hohenstein P, Kimber CH, Tenesa A, Donnelly LA, Fairbanks LD, Aringer M, McKeigue PM, Ralston SH, Morris AD, Rudan P, Hastie ND, Campbell H, Wright AF (2008) SLC2A9 is a newly identified urate transporter influencing serum urate concentration, urate excretion and gout. Nat Genet 40:437-442

Wang Z, Rolish ME, Yeo G, Tung V, Mawson M, Burge CB (2004) Systematic identification and analysis of exonic splicing silencers. Cell 119:831-845

Ward LM, Rauch F, Travers R, Chabot G, Azouz EM, Lalic L, Roughley PJ, Glorieux FH (2002) Osteogenesis imperfecta type VII: an autosomal recessive form of brittle bone disease. Bone 31:12-18

Woodward OM, Kottgen A, Coresh J, Boerwinkle E, Guggino WB, Kottgen M (2009) Identification of a urate transporter, ABCG2, with a common functional polymorphism causing gout. Proc Natl Acad Sci U S A 106:10338-10342

Yeo GW, Coufal NG, Liang TY, Peng GE, Fu XD, Gage FH (2009) An RNA code for the FOX2 splicing regulator revealed by mapping RNA-protein interactions in stem cells. Nat Struct Mol Biol 16:130-137

Yi X, Liang Y, Huerta-Sanchez E, Jin X, Cuo ZX, Pool JE, Xu X, Jiang H, Vinckenbosch N, Korneliussen TS, Zheng H, Liu T, He W, Li K, Luo R, Nie X, Wu H, Zhao M, Cao H, Zou J, Shan Y, Li S, Yang Q, Asan, Ni P, Tian G, Xu J, Liu X, Jiang T, Wu R, Zhou G, Tang M, Qin J, Wang T, Feng S, Li G, Huasang, Luosang J, Wang W, Chen F, Wang Y, Zheng X, Li Z, Bianba Z, Yang G, Wang X, Tang S, Gao G, Chen Y, Luo Z, Gusang L, Cao Z, Zhang Q, Ouyang W, Ren X, Liang H, Zheng H, Huang Y, Li J, Bolund L, Kristiansen K, Li Y, Zhang Y, Zhang X, Li R, Li S, Yang H, Nielsen R, Wang J, Wang J (2010) Sequencing of 50 human exomes reveals adaptation to high altitude. Science 329:75-78

Zhang XH, Chasin LA (2004) Computational definition of sequence motifs governing constitutive exon splicing. Genes Dev 18:1241-1250

Zhang XH, Kangsamaksin T, Chao MS, Banerjee JK, Chasin LA (2005) Exon inclusion is dependent on predictable exonic splicing enhancers. Mol Cell Biol 25:7323-7332

Figure legends

Fig. 1 Pedigrees, haplotypes, and genotypes of the Japanese (F1 and F4), Italian (F2), and Canadian (F3) families. Patients in F1, F2, and F3 have c.3235G>A predicting p.G1079S in *COL1A1*. A patient in F4 has c.577G>T predicting p.G193C in *COL1A2*. Closed symbols indicate patients with OI and with hyperuricemia. Half-shaded symbols represent OI without hyperuricemia. Asterisks indicate that DNA sample is not available for our studies. Clinical subtypes are all type I except for the Canadian father (V-1) who exhibits type IV. In F1, hyperuricemia cosegregates with OI. Genotypes of three microsatellite markers (D17S1293, -16Mbp; D17S1319, -14kbp; and D17S788, 2Mb) flanking *COL1A1* and a SNP (rs2075554) in intron 11 of *COL1A1* are indicated for all the available members in F1, F2, and F3. F1, F2, and F3 carry their unique haplotypes (shown by solid, dotted, and broken boxes, respectively). The D17S1293 genotype in F3 is not informative and is not boxed. Genotypes of hyperuricemia-associated SNPs (rs2231142, rs3825016, and rs11231825) are indicated at the bottom of each pedigree tree.

Fig. 2 Splicing assays of *COL1A1* minigenes in HEK293 cells. **a** Positions and phenotypes of OI mutations in *COL1A1* exon 45. Mutations above the wild-type sequence exhibit non-lethal phenotypes, whereas those below the sequence cause a lethal phenotype. **b** Schematic representation of *COL1A1* minigenes. Sequences of mutant minigenes are indicated below. Substituted nucleotides are shown in bold. Predicted gain and loss of splicing *cis*-elements by ESEfinder (Cartegni et al. 2003) are indicated by solid and dotted underlines, respectively. **c** RT-PCR of minigenes introduced into HEK293 cells. All constructs show a single fragment of 336 bp, indicating that *COL1A1* exon 45 is not skipped in any constructs. Untransfected cells are used as a negative control (NC).

Fig. 3 Conservation of 21 amino-acid segments encoded by *ZPBP2* and *GPATCH8* in mammals. Locations of non-synonymous variants identified in the Japanese family (F1) are boxed. Amino acids identical to human are shaded. **a** c.206C>T predicts p.T69I in *ZPBP2*. T69 is not conserved in rat and opossum. A SNP rs35591738 predicts p.P68A, and a SNP rs34272593 induces a frameshift. **b** c.2935G>C predicts p.A979P in *GPATCH8*. The mutation is located at the C-terminal end of the serine-rich region.

Table 1 Affected putative splicing *cis*-elements in *COL1A1* exon 45 predicted by ESEfinder, ESRsearch, and PESXs

Sequence variation	Normal allele	Variant allele	Predicted effect	Score[d]		Putative *trans*-factor
				Normal	Variant	
rs1800215	CC**G**CCGG	CC**A**CCGG[a]	Gain	1.622	4.231	SRp40
rs1800217	CTGT**T**GGC	CTGT**C**GGC[c]	Gain		n.a.	
c.3226G>A	CGCC**G**G	CGCC**A**G[b]	Gain		n.a.	
	CC**G**GTCCT	CC**A**GTCCT[c]	Gain		n.a.	
c.3226G>A+rs1800215	CC**G**CC**G**G	CC**A**CC**A**G[a]	Gain	1.622	3.663	SRp40
c.3226G>T	CGCC**G**G	CGCC**T**G[b]	Gain		n.a.	
c.3226G>T+rs1800215	CC**G**CC**G**G	CC**A**CC**T**G[a]	Loss	3.498	0.571	SF2/ASF
c.3235G>A	CTGTC**G**G	CTGTC**A**G[a]	Loss	2.492	0.713	SF2/ASF
	CTGTC**G**GC	CTGTC**A**GC[c]	Loss		n.a.	
	TGTC**G**GC	TGTC**A**GC[a]	Gain	1.058	3.613	SRp40
	GTC**G**GC	GTC**A**GC[b]	Gain		n.a.	
	C**G**GCCCTG	C**A**GCCCTG[c]	Gain		n.a.	
c.3244G>T	**G**GCGCCCG	**T**GCGCCCG[a]	Loss	3.109	1.059	SC35
	GGCGCC	**T**GCGCC[a]	Gain	0.721	3.531	SRp55
c.3244G>T+rs1800217	TGT**T**G**G**C	TGT**C**T**G**C[a]	Gain	-1.326	3.367	SRp40
c.3253G>A	CGT**G**GC	CGT**A**GC[a]	Loss	2.940	2.331	SRp55

Variant nucleotides are shown in bold and underlined.

[a]ESEfinder, [b]ESRsearch, and [c]PESXs

[d]Default threshold values employed by ESEfinder are SRp40 = 2.67, SF2/ASF = 1.867, SC35 = 2.383, and SRp55 = 2.676; n.a., not applicable.

Table 2 Splice site strength of *COL1A1* exon 45 predicted by the NetGene2 and the Splice Site Prediction by Neural Network

Sequence variation	NetGene2 Confidence		Splice Site Prediction by Neural Network Score	
	Acceptor	Donor	Acceptor	Donor
Wild type	0.97	0.93	0.98	0.95
rs1800215	-	-	-	-
rs1800217	-	-	-	-
c.3226G>A	-	0.89	-	-
c.3226G>A+rs1800215	0.94	0.89	-	-
c.3226G>A+rs1800217	-	0.89	-	-
c.3226G>T	0.94	0.87	-	-
c.3226G>T+rs1800215	0.94	0.86	-	-
c.3226G>T+rs1800217	0.94	0.87	-	-
c.3235G>A	0.94	0.87	-	-
c.3235G>A+rs1800215	0.94	0.86	-	-
c.3235G>A+rs1800217	0.94	0.87	-	-
c.3244G>T	0.94	0.86	-	-
c.3244G>T+rs1800215	0.94	0.86	-	-
c.3244G>T+rs1800217	0.94	0.86	-	-
c.3253G>A	0.94	0.88	0.52[a]	-
c.3253G>A+rs1800215	0.94	0.87	0.52[a]	-
c.3253G>A+rs1800217	-	0.89	-	-

Hyphens represent being identical to the wild-type.

[a]In addition to the native splice acceptor site of 0.98, a cryptic splice acceptor site 'AG' is generated at c.3253_3254.

Table 3 Twelve SNPs identified by exome resequensing in 5 out of 10 genes associated with hyperuricemia

Ch	Gene	Position	Nuc.	Amino acid	AF	dbSNP	II-2	II-3	VIII-2
1	*AGL*	100,336,361	C>T	Syn.	0.7	rs2230306	T/T	-/T	-/T
4	*ABCG2*[b]	89,034,551	G>A	Syn.	0.02	rs35622453	-/-	-/-	-/A
		89,052,323	C>A	Q141K	0.31	rs2231142	-/A	A/A	-/-
		89,061,114	G>A	V12M	0.19	rs2231137	-/A	-/-	-/A
4	*SLC2A9*[b]	9,909,923	C>T	P350L	0.33	rs2280205	-/T	-/T	-/-
		9,922,130	G>A	R294H	0.72	rs3733591	-/A	-/-	-/A
		9,998,440	G>A	Syn.	0.54	rs10939650	-/A	A/A	-/A
		10,022,981	G>A	G25R	0.43	rs2276961	-/A	-/A	-/-
		10,027,542	G>A	A17T	0.06	rs6820230	-/-	-/A	-/A
11	*SLC22A12*[b]	64,359,286	C>T	Syn.	0.21	rs3825016	-/T	T/T	-/T
		64,360,274	C>T	Syn.	0.81	rs11231825	-/T	-/-	-/T
12	*PFKM*		n.d.						
16	*UMOD*[b]		n.d.						
17	*G6PC*		n.d.						
X	*HPRT1*[a]		n.d.						
X	*PRPS1*[a]		n.d.						
X	*MAOA*	43,591,036	G>T	Syn.	0.3	rs6323	-/-	T/T	T/T

The gene is associated with purine metabolism (a) or renal excretion of urate (b).

Hyphens in the patients' genotypes mean identical to the reference nucleotides.

Syn., synonymous nucleotide change; AF, allelic frequency of the changed nucleotide; n.d., no SNPs are detected.

Supplementary Table 1 PCR primers used for microsatellite analysis

Gene	Marker	Location		Sequence (5'→3')
COL1A1				
	D17S1293	-16 Mb	Forward	TGGAGGCTAGGAGTTTTCCT
			Reverse	GGAGGCAGTGAGTTGTGATT
	D17S1319	-14 Mb	Forward	TCCCATGCTGCTTCCTATCT
			Reverse	ACTCTGTTGCCCTCTTGTGG
	D17S788	+2 Mb	Forward	CTAGGCAGCCACTACCAAAT
			Reverse	CAGCATCTTTGCTATAAGCATC
COL1A2				
	AB499843	-17 kb	Forward	GCTTGGAAGACACTGCTGAA
			Reverse	CAGACTGGCCACTTTTTCAAG
	AB499844	+29 kb	Forward	TGATCACAACCCAATGAATAAAA
			Reverse	TCCCGTCTGCATCAATTACT
	AB499845	+123 kb	Forward	GCTGGTTATTGGATGTGAGACA
			Reverse	CTCCTCTCCCCTGTCCTTTT

Supplementary Table 2 Fourteen genes involved in urate metabolisms and excretion

Ch	Gene	Position	Nuc.	Amino acid	AF	dbSNP	II-2	II-3	VIII-2
1	*AMPD1*[a]		n.d.						
1	*AMPD2*[a]		n.d.						
2	*XDH*[a]	31,569,660	A>C	N1109T	0.08	rs45547640	-/C	-/-	-/-
		31,571,786	T>C	Syn.	0.88	rs1884725	C/C	C/C	-/C
		31,589,847	C>T	Syn.	0.28	rs2295475	T/T	-/T	-/-
		31,606,670	C>T	Syn.	0.07	rs4407290	-/-	-/T	-/T
		31,611,143	G>A	G172R	0.04	rs45523133	-/A	-/A	-/A
6	*SLC17A1*[b]	25,813,150	C>T	T269I	0.83	rs1165196	-/T	-/T	-/T
11	*SLC22A11*[b]		n.d.						
11	*AMPD3*[a]		n.d.						
14	*PNP*[a]		n.d.						
16	*APRT*[a]		n.d.						
17	*PRPSAP1*[a]		n.d.						
17	*PRPSAP2*[a]		n.d.						
18	*MOCOS*[a]		n.d.						
20	*ADA*[a]		n.d.						
22	*ADSL*[a]		n.d.						
X	*PRPS2*[a]		n.d.						

The gene is associated with purine metabolism (a) or renal excretion of urate (b).

Hyphens in the patients' genotypes mean identical to the reference nucleotides.

Syn., synonymous nucleotide change; AF, allelic frequency of the changed nucleotide; n.d., no SNPs are detected.

Japanese family (F1)

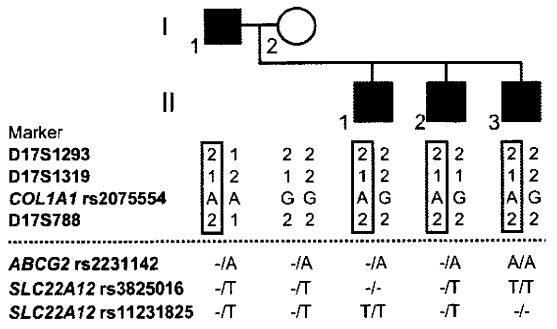

Italian family (F2)

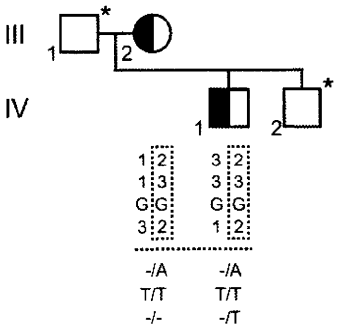

Canadian family (F3)

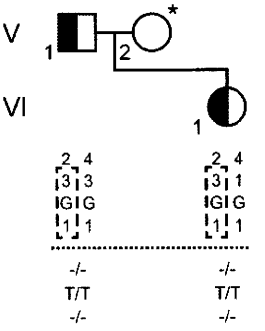

Japanese family (F4)

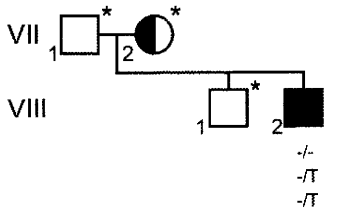

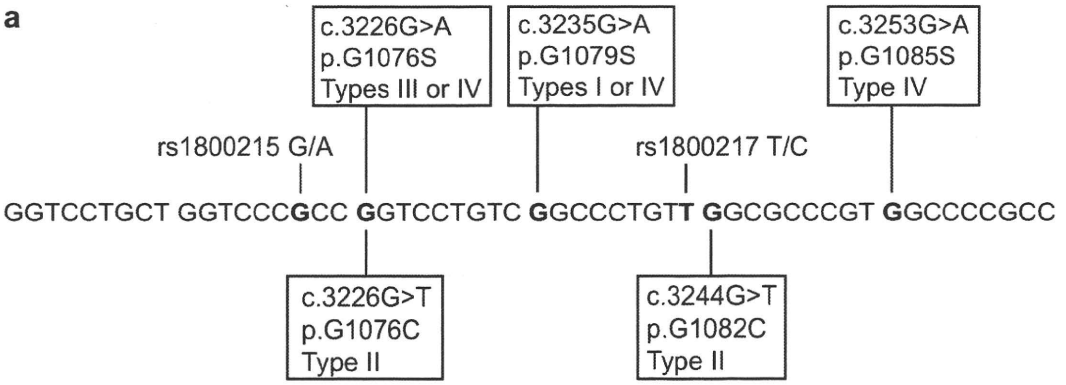

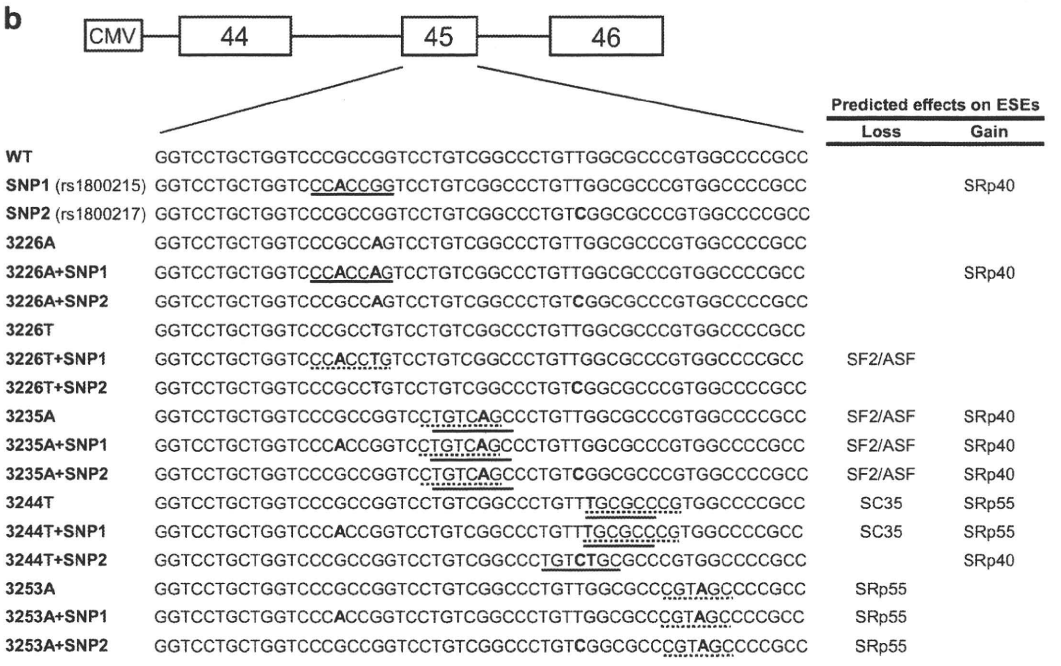

		Predicted effects on ESEs	
		Loss	Gain
WT	GGTCCTGCTGGTCCCGCCGGTCCTGTCGGCCCTGTTGGCGCCCGTGGCCCCGCC		
SNP1 (rs1800215)	GGTCCTGCTGGTCCCACCGGTCCTGTCGGCCCTGTTGGCGCCCGTGGCCCCGCC		SRp40
SNP2 (rs1800217)	GGTCCTGCTGGTCCCGCCGGTCCTGTCGGCCCTGT**C**GGCGCCCGTGGCCCCGCC		
3226A	GGTCCTGCTGGTCCCGCC**A**GTCCTGTCGGCCCTGTTGGCGCCCGTGGCCCCGCC		
3226A+SNP1	GGTCCTGCTGGTCCCACCAGTCCTGTCGGCCCTGTTGGCGCCCGTGGCCCCGCC		SRp40
3226A+SNP2	GGTCCTGCTGGTCCCGCC**A**GTCCTGTCGGCCCTGT**C**GGCGCCCGTGGCCCCGCC		
3226T	GGTCCTGCTGGTCCCGCCTGTCCTGTCGGCCCTGTTGGCGCCCGTGGCCCCGCC		
3226T+SNP1	GGTCCTGCTGGTCCCACCTGTCCTGTCGGCCCTGTTGGCGCCCGTGGCCCCGCC	SF2/ASF	
3226T+SNP2	GGTCCTGCTGGTCCCGCCTGTCCTGTCGGCCCTGT**C**GGCGCCCGTGGCCCCGCC		
3235A	GGTCCTGCTGGTCCCGCCGGTCCTGTCAGCCCTGTTGGCGCCCGTGGCCCCGCC	SF2/ASF	SRp40
3235A+SNP1	GGTCCTGCTGGTCCC**A**CCGGTCCTGTCAGCCCTGTTGGCGCCCGTGGCCCCGCC	SF2/ASF	SRp40
3235A+SNP2	GGTCCTGCTGGTCCCGCCGGTCCTGTCAGCCCTGT**C**GGCGCCCGTGGCCCCGCC	SF2/ASF	SRp40
3244T	GGTCCTGCTGGTCCCGCCGGTCCTGTCGGCCCTGTTTGCGCCCGTGGCCCCGCC	SC35	SRp55
3244T+SNP1	GGTCCTGCTGGTCCC**A**CCGGTCCTGTCGGCCCTGTTTGCGCCCGTGGCCCCGCC	SC35	SRp55
3244T+SNP2	GGTCCTGCTGGTCCCGCCGGTCCTGTCGGCCCTGT**CT**GCGCCCGTGGCCCCGCC		SRp40
3253A	GGTCCTGCTGGTCCCGCCGGTCCTGTCGGCCCTGTTGGCGCCCGTAGCCCCGCC	SRp55	
3253A+SNP1	GGTCCTGCTGGTCCC**A**CCGGTCCTGTCGGCCCTGTTGGCGCCCGTAGCCCCGCC	SRp55	
3253A+SNP2	GGTCCTGCTGGTCCCGCCGGTCCTGTCGGCCCTGT**C**GGCGCCCGTAGCCCCGCC	SRp55	

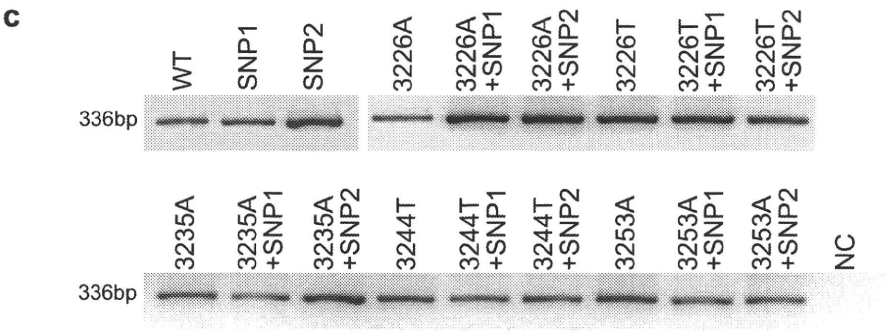

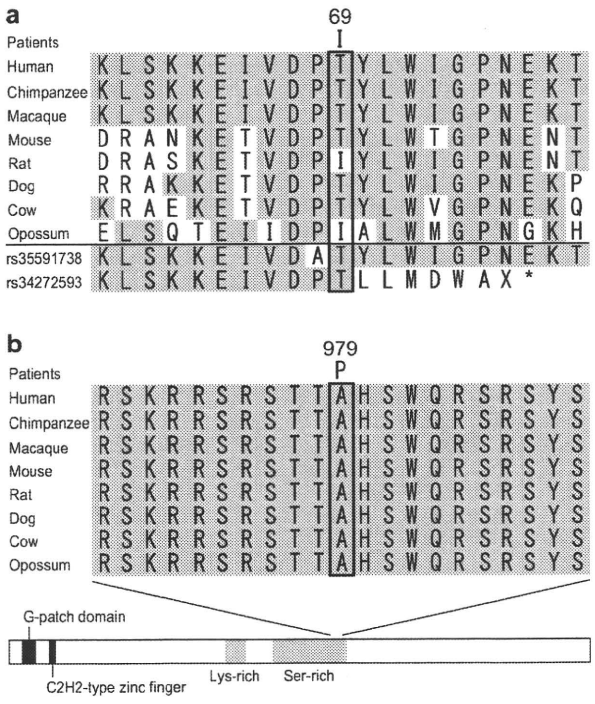
a
69
I
Patients
Human K L S K K E I V D P T Y L W I G P N E K T
Chimpanzee K L S K K E I V D P T Y L W I G P N E K T
Macaque K L S K K E I V D P T Y L W I G P N E K T
Mouse D R A N K E T V D P T Y L W T G P N E N T
Rat D R A S K E T V D P I Y L W I G P N E N T
Dog R R A K K E T V D P T Y L W I G P N E K P
Cow K R A E K E T V D P T Y L W V G P N E K Q
Opossum E L S Q T E I I D P I A L W M G P N G K H
rs35591738 K L S K K E I V D A T Y L W I G P N E K T
rs34272593 K L S K K E I V D P T L L M D W A X *
b
979
P
Patients
Human R S K R R S R S T T A H S W Q R S R S Y S
Chimpanzee R S K R R S R S T T A H S W Q R S R S Y S
Macaque R S K R R S R S T T A H S W Q R S R S Y S
Mouse R S K R R S R S T T A H S W Q R S R S Y S
Rat R S K R R S R S T T A H S W Q R S R S Y S
Dog R S K R R S R S T T A H S W Q R S R S Y S
Cow R S K R R S R S T T A H S W Q R S R S Y S
Opossum R S K R R S R S T T A H S W Q R S R S Y S
G-patch domain
C2H2-type zinc finger
Lys-rich
Ser-rich

Anti-MuSK autoantibodies block binding of collagen Q to MuSK

Yu Kawakami, BSc;[1] Mikako Ito, PhD;[1] Masaaki Hirayama, MD, PhD;[3] Ko Sahashi, MD, PhD;[2] Bisei Ohkawara, PhD;[1] Akio Masuda, MD, PhD;[1] Hiroshi Nishida, MD, PhD;[4] Naoki Mabuchi, MD, PhD;[5] Andrew G. Engel, MD; [6] Kinji Ohno, MD, PhD[1]

[1]Division of Neurogenetics, Center for Neurological Diseases and Cancer, Nagoya University Graduate School of Medicine, Nagoya, Japan
[2]Department of Neurology, Aichi Medical University, Aichi, Japan
[3]Department of Pathophysiological Laboratory Sciences, Nagoya University Graduate School of Medicine, Nagoya, Japan
[4]Department of Neurology, Gifu Prefectural General Medical Center, Gifu, Japan
[5]Department of Neurology, Okazaki City Hospital, Okazaki, Japan
[6]Department of Neurology, Mayo Clinic, Rochester, Minnesota

Address correspondence to Dr. Ohno, Division of Neurogenetics, Center for Neurological Diseases and Cancer, Nagoya University Graduate School of Medicine, 65 Tsurumai, Showa-ku, Nagoya 466-8550, Japan
e-mail: ohnok@med.nagoya-u.ac.jp

E-mails accounts

Yu Kawakami	kawakami.yuu@med.nagoya-u.ac.jp
Mikako Ito	ito@med.nagoya-u.ac.jp
Masaaki Hirayama	hirasan@med.nagoya-u.ac.jp
Ko Sahashi	kssahashi@flute.ocn.ne.jp
Bisei Ohkawara	biseiohkawara@med.nagoya-u.ac.jp
Akio Masuda	amasuda@med.nagoya-u.ac.jp
Hiroshi Nishida	41151@gifu-hp.jp
Naoki Mabuchi	mrchm4852001@yahoo.co.jp
Andrew G. Engel	age@mayo.edu
Kinji Ohno	ohnok@med.nagoya-u.ac.jp

Glossaries

AChE = acetylcholinesterase; AChR = acetylcholine receptor; ColQ = collagen Q; Ct = control; LRP4 = low-density lipoprotein receptor-related protein 4; MG = myasthenia gravis; MuSK = muscle-specific receptor tyrosine kinase; NMJ = neuromuscular junction; Pt = patient.

Word counts

Number of words: Abstract, 249 words; Text, 2842 words

Number of characters: Title, 60 chars

Number of figures: 4 figures (3 color figures); Number of Tables: 0

Number of references: 39 references

There is one supplementary table.

Keywords

Myasthenia gravis, MuSK, and ColQ

Study funding

Supported by the MEXT and MHLW of Japan, NIH (NS6277), and the Muscular Dystrophy Association.

Disclosure statements

This study is supported by a Grant-in-Aid from the Ministry of Education, Culture, Sports, Science, and Technology of Japan; a Grant-in-Aid from the Ministry of Health, Labor, and Welfare of Japan; a research grant from the National Institute of Neurological Disorders and Stroke (NS6277); and a research grant from the Muscular Dystrophy Association.

Dr. Kawakami designed and conducted experiments, and wrote a paper. He has no financial disclosure.
Dr. Ito designed and conducted experiments. She has no financial disclosure.
Dr. Hirayama conducted experiments. He has no financial disclosure.
Dr. Sahashi diagnosed a patient and conceived studies. He has no financial disclosure.
Dr. Ohkawara designed experiments. She has no financial disclosure.
Dr. Masuda designed experiments. He has no financial disclosure.
Dr. Nishida diagnosed a patient and conceived studies. He has no financial disclosure.
Dr. Mabuchi diagnosed a patient and conceived studies. He has no financial disclosure.
Dr. Engel diagnosed a patient, conceived studies, designed experiments, and wrote a paper. He serves as an Associate Editor of Neurology; receives publishing royalties for Myology 3rd ed. (McGraw-Hill, 2004); and has received research support from the NIH and the Muscular Dystrophy.
Dr. Ohno conceived studies, designed experiments, and wrote a paper. He has received Grants-in-Aids from the MEXT and the MHLW of Japan.

Abstract

Objective: MuSK antibody-positive myasthenia gravis (MG) accounts for 5-15% of autoimmune MG. MuSK mediates the agrin-signaling pathway and also anchors the collagenic tail subunit (ColQ) of acetylcholinesterase. The exact molecular target of MuSK-IgG, however, still remains elusive. As acetylcholine receptor (AChR) deficiency is typically mild and as cholinesterase inhibitors are generally ineffective, we asked if MuSK-IgG interferes with binding of ColQ to MuSK.

Methods: We used three assays: *In vitro* overlay of the human ColQ-tailed acetylcholinesterase (AChE) to muscle sections of *Colq*-/- mice; *in vitro* plate-binding assay to quantitate binding of MuSK to ColQ and to LRP4; and passive transfer of MuSK-IgG to mice.

Results: *In vitro* overlay assay revealed that MuSK-IgG blocks binding of ColQ to the neuromuscular junctions. *In vitro* plate-binding assay showed a dose-dependent block by MuSK-IgG of the binding of MuSK to ColQ but not to LRP4. Passive transfer of MuSK-IgG to mice reduced the size and density of ColQ to ~10% of controls and had a lesser effect on the size and density of AChR and MuSK.

Conclusions: As lack of ColQ compromises agrin-mediated AChR clustering in *Colq*-/- mice, a similar mechanism may lead to AChR deficiency in MuSK-MG patients. Our experiments also predict partial AChE deficiency in MuSK-MG patients, but AChE is not reduced in biopsied NMJs. In humans, binding of ColQ to MuSK may be dispensable for clustering ColQ, but is required for facilitating AChR clustering. Further studies will be required to elucidate the basis of this paradox.

Introduction

During development of the neuromuscular junction (NMJ), neural agrin released from the nerve terminal binds to the postsynaptic transmembrane protein LRP4[1, 2]. Dimerized LRP4 forms a heterotetramer with the dimerized muscle-specific receptor tyrosine kinase (MuSK)[3]. MuSK together with Dok-7 promotes clustering of acetylcholine receptor (AChR) on the junctional folds by rapsyn[4]. The clustering effect of MuSK is mediated by distinct pathways involving Rho GTPase[5].

Acetylcholine released from the nerve terminal is rapidly hydrolyzed by acetylcholinesterase (AChE) at the NMJ. Three tetramers of catalytic subunits of AChE are linked to ColQ, the triple helical collagenic subunit[6]. ColQ-tailed AChE is anchored to the synaptic basal lamina by two mechanisms: First, two sets of heparan sulfate proteoglycan (HSPG) residues in the collagen domain of ColQ[7] bind to heparin sulfate proteoglycans, such as perlecan[8]. Second, the C-terminal domain of ColQ binds to MuSK[9].

Five to fifteen percent of myasthenia gravis (MG) patients carry antibodies against MuSK (MuSK-IgG)[10]. MuSK-MG patients often exhibit prominent weakness and atrophy of the oculobulbar muscles[11]. MuSK-MG patients favorably respond to immunotherapy, but usually do not respond to or are even worsened by cholinesterase inhibitors[12-15]. In contrast to complement-activating IgG1 and IgG3 in AChR antibodies, MuSK antibodies are largely IgG4 that do not activate complement, and complement deposits at the NMJ are sparse[16-18]. The exact target of MuSK-IgG, however, remains elusive. We thus examined an effect of MuSK-IgG on an interaction between ColQ and MuSK by *in vitro* and *in vivo* assays, and found that MuSK-IgG blocks this interaction.

Methods

Patients. We obtained serum from four MuSK-MG patients (Pts. 1-4) and a patient with limb-girdle muscular dystrophy as a control (Ct. 1). For Pts. 1, 3, 4, and Ct. 1, we obtained 10 ml peripheral blood. For Pt. 2, we obtained residual fluid of plasmapheresis. We also obtained expired fresh frozen plasma (Ct. 2) from Dr. Isao Takahashi at the Aichi Red Cross Blood Center under the institutional approval. All human studies were performed under the IRB approvals of the Nagoya University Graduate School of Medicine and the Mayo Clinic, and written informed consents were obtained from each patient and a control.

Ages and genders of Pts. 1-4 were a 48-y.o. female, a 30-y.o. female, a 59-y.o. male, and a 45-y.o. female, respectively. The titers of anti-MuSK antibodies of Pts. 1-3 were 22.0 nM, 11.2 nM, 0.12 nM, respectively, where the normal range was less than 0.01 nM. Pt. 4 was positive for anti-MuSK antibody, but the titer was not determined.

Plasmids. We previously made a CMV-based mammalian expression vectors, pTargeT-*COLQ* and pTargeT-*ACHE*[19]. To generate hMuSKect-myc, we subcloned the

extracellular domain (a.a. 1-393) of human *MUSK* cDNA (Open Biosystems) into a mammalian expression vector pAPtag-5 (GenHunter) at the *Nhe*I and *Xho*I sites upstream of a myc epitope. For hLRP4N-FLAG, the extracellular domain (a.a. 1-1722) of human *LRP4* cDNA (Open Biosystems) was subcloned into *Hin*dIII and *Xba*I sites upstream of a 3xFLAG epitope of a mammalian expression vector p3XFLAG-CMV-14 (Sigma Aldrich).

Preparation of recombinant human ColQ-tailed AChE. We prepared human ColQ-tailed AChE for *in vitro* overlay assay and for *in vitro* plate-binding assay. Both pTargeT-*COLQ* and pTargeT-*ACHE* were transfected into HEK293 cells in a 10-cm dish using the calcium phosphate method as described elsewhere[20]. Proteins were extracted from the cells in Tris-HCl buffer [50 mM Tris-HCl (pH 7.0), 0.5% Triton X-100, 0.2 mM EDTA, leupeptin (2 μg/ml), and pepstatin (1 μg/ml)] containing 1 M NaCl. The extracts containing ColQ-tailed AChE were diluted to Tris-HCl buffer containing 0.2 M NaCl and loaded onto the HiTrap Heparin HP columns (GE Healthcare). The columns were washed with 5 volumes of Tris-HCl buffer containing 0.2 M NaCl. ColQ-tailed AChE was then eluted with Tris-HCl buffer containing 1 M NaCl. The eluate was concentrated with an Amicon Ultra-4 Centrifugal Filter (50 K) (Millipore) to 12-Ellman units per ml. The units were normalized with the Torpedo-derived AChE (C2888, Sigma-Aldrich).

Preparation of hMuSKect-myc and hLRP4N-FLAG. We prepared hMuSKect-myc and hLRP4N-FLAG for *in vitro* plate-binding assays. A construct carrying either hMuSKect-myc or hLRP4N-FLAG was introduced into HEK293 cells in a 10-cm dish using the calcium phosphate method as above. The hMuSKect-myc was purified with the c-myc-Tagged Protein Mild Purification Kit ver. 2 (MBL). The hLRP4N-FLAG was purified with the Anti-DYKDDDDK-tag Antibody Beads (Wako). Purified hMuSKect-myc and hLRP4N-FLAG were detected by anti-myc antibody (9E10, Abcam) and anti-FLAG antibody (M2, Sigma-Aldrich), respectively (data not shown). We also detected hMuSKect-myc by SDS-PAGE followed by protein staining with the Oriole Fluorescent Gel Stain (Bio-Rad).

Purification of plasma IgG. We purified IgG as described elsewhere[21] with minor modifications. Plasma was adjusted to pH 8.0 with 1 M NaOH. While stirring one volume of plasma, we slowly added 3.5 volumes of 0.4% rivanol (Tokyo Chemical Industries) in water for 30 min. The solution was left overnight at RT, and a tenacious yellow precipitate was removed. The supernatant was filtered through Whatman #1 paper to remove residual precipitates. We added 8 g of activated charcoal (Wako Chemicals) for 100 ml of the IgG solution and incubated overnight at 4 °C to remove rivanol. We then slowly added an equal amount of saturated ammonium sulfate, and again incubated overnight at RT to precipitate crude IgG. We centrifuged the solution at 3,000 x *g* for 30 min, and added saline to the

precipitate to form a slurry, which was then transferred to a dialysis tube (Spectra/Por MWCO 50,000, Spectrum Laboratories). The solution was dialyzed in saline at 4 °C for 3 hrs. Thereafter, the solution was dialyzed in PBS at 4 °C for 2 hrs and then overnight. We removed residual charcoals by filtering through a 0.22-μm Millex-GP filter (Millipore), and concentrated IgG using Amicon Ultra 50K (Millipore). We confirmed purity of isolated IgG by 6% SDS-PAGE under a non-reducing condition. We also reduced IgG in 4% 2-mercaptoethanol and fractionated the heavy and light chains by 10% SDS-PAGE.

Incubation of purified IgG to a muscle section of *Colq-/-* mice. Quadriceps muscles of *Colq-/-* mice[22] were frozen in the liquid nitrogen-cooled isopentane. We prepared 10-μm thick sections with a Leica CW3050-4 cryostat at -20 °C. We blocked non-specific binding of a muscle section with the blocking buffer that contains 5% sheep serum in PBS at RT for 2 hrs. We suspended the purified IgG in the blocking buffer at 50 μg/ml, and overlaid it on a muscle section at 4 °C overnight. Human IgG was detected by FITC-labeled anti-human IgG antibody (02-10-06, KPL). AChR was detected by Alexa594-labeled α-bungarotoxin (Molecular Probes). Signals were examined with BX60 (Olympus) or BZ-9000 (Keyence). Studies of *Colq-/-* mice were approved by the Animal Care and Use Committee of the Nagoya University Graduate School of Medicine.

***In vitro* overlay assay.** The overlay binding method was essentially as previously described[23]. We overlaid 600 μg IgG of patients at 4 °C overnight before adding 120-milli-Ellman units of ColQ-tailed AChE.

***In vitro* plate-binding assay for quantifying ColQ-MuSK interaction.** The Maxi-Sorp Immuno Plate (Nunc) was coated with 0.15 μg of purified hMuSKect-myc at 4 °C overnight and then incubated with a blocking buffer that contained 50 mM Tris-HCl (pH 7.4), 0.5% BSA, 0.5% ovalbumin, and 0.5 M NaCl at RT for 1 hr. The wells were incubated with 1 pg to 100 μg of IgG of Cts.1-2 and Pts. 1-4 at 4 °C for 6 hrs. We added 0.12-Ellman units of ColQ-tailed AChE as described above. We then quantified the bound ColQ-tailed AChE by the Ellman method in the presence of 5×10^{-5} M ethopropazine[19]. Each time before we moved to the next step, we washed the plate with PBS three times. The washing steps were thus repeated four times.

***In vitro* plate-binding assay for quantifying LRP4-MuSK interaction.** The Maxi-Sorp Immuno Plate was coated with 0.15 μg of purified hMuSKect-myc as described above, and then blocked with 1% BSA in PBS at RT for 1 hr. The wells were incubated with 1 pg to 100 μg of IgG of Ct. 2 and Pt. 2 at 4 °C for 6 hrs. We added 0.12 μg of purified hLRP4N-FLAG on each well at RT for 2 hours. Bound hLRP4N-FALG was quantified by anti-FLAG-HRP